Applied Surface Science 419 (2017) 758–763

Contents lists available at ScienceDirect

Applied Surface Science

journal homepage: www.elsevier.com/locate/apsusc

Full Length Article

Thermal atomic layer deposition of In_2O_3 thin films using dimethyl(*N*-ethoxy-2,2-dimethylcarboxylicpropanamide)indium and H_2O

Raphael Edem Agbenyeke[a,b], Eun Ae Jung[a,c], Bo Keun Park[a,b], Taek-Mo Chung[a,b], Chang Gyoun Kim[a,b,*], Jeong Hwan Han[a,b,*]

[a] Division of Advanced Materials, Korea Research Institute of Chemical Technology (KRICT), 141 Gajeong-Ro, Yuseong-Gu, Daejeon 34114, Republic of Korea
[b] Department of Chemical Convergence Materials, University of Science and Technology (UST), 217, Gajeong-Ro, Yuseong-Gu, Deajeon 34113, Republic of Korea
[c] Department of Chemistry, Sungkyunkwan University, Suwon 16419, Republic of Korea

ARTICLE INFO

Article history:
Received 17 January 2017
Received in revised form 28 April 2017
Accepted 8 May 2017
Available online 10 May 2017

Keywords:
Atomic layer deposition
$Me_2In(EDPA)$
In_2O_3
Oxide semiconductor

ABSTRACT

Indium oxide (In_2O_3) thin films were deposited by atomic layer deposition using dimethyl(*N*-ethoxy-2,2-dimethylcarboxylicpropanamide)indium ($Me_2In(EDPA)$) and H_2O as the In-precursor and reactant, respectively. The In_2O_3 films exhibited a saturated growth rate of 0.083 nm/cycle at a deposition temperature of 300 °C. Porous and amorphous films were grown at 150 °C, whereas dense polycrystalline films were deposited at higher deposition temperatures of 200–300 °C. XPS analysis revealed negligible carbon and nitrogen impurities incorporation within the films. The estimated bandgap of the In_2O_3 films by spectroscopic ellipsometry and UV–vis spectroscopy was about 3.7 eV and the increase in refractive index with deposition temperature from 150 to 300 °C indicated that dense films were grown at higher temperatures. The high transmittance (>94% in visible light) and good electrical properties (resistivity ~1.2–7 mΩ cm, Hall mobility ~28–66 $cm^2/V s$) of the In_2O_3 films make them a viable option for optoelectronic applications.

1. Introduction

Indium oxide (In_2O_3) is a III–VI binary oxide semiconductor material with a cubic crystal structure and a wide optical band gap of 3–4 eV [1]. It shows high transparency to visible light and possesses excellent electrical properties, which makes it an essential material in microelectronics [2], optoelectronics [3], photovoltaics [1,2,4], and gas sensors [3,5,6]. In the doped form as tin-doped In_2O_3, it has been employed as transparent pixel electrode in display applications such as liquid crystal displays and organic light-emitting diodes [6].

Owing to the vast applications and hence high demand of In_2O_3, many attempts have been made to grow it in different morphologies/shapes including nanorods [5], nanowires [7], and thin films [8,9], using various deposition techniques such as sputtering [10], pulsed laser deposition [11], metal-organic chemical vapor deposition [5], and atomic layer deposition (ALD) [4,8,9,12]. The properties of oxide semiconductor thin films strongly depend on the thickness and morphology; hence the latter is a much preferred route to deposit smooth In_2O_3 thin films as it allows excellent control over film thickness due to its unique layer by layer deposition manner resulting in uniform conformal coatings on complex structured substrates.

ALD however is a relatively slow deposition process particularly when the surface reactions between the chemisorbed precursor and the reactant gas are not facile, thus resulting in low growth rates. ALD growth of In_2O_3 thin films has been explored with various combinations of In-precursors and reactants but limited successes have been reported. For instance, In_2O_3 ALD studies using $In(tmhd)_3$ (tmhd = 2,2,6,6-tetramethylheptane-3,5-dionate), $In(hfac)_3$ (hfac = hexafluoroacetylacetonate), and $In(acac)_3$ (acac = acetylactonate) with H_2O as reactant recorded almost no film growth owing to relatively low reactivity of the β-diketonate ligand containing In-precursors [8]. Studies with trimethylindium and H_2O have also been quite inconsistent, either resulting in no film growth [12,13] or non-self-limiting

* Corresponding authors at: Division of Advanced Materials, Korea Research Institute of Chemical Technology (KRICT), 141 Gajeong-Ro, Yuseong-Gu, Daejeon 34114, Republic of Korea.
E-mail addresses: cgkim@krict.re.kr (C.G. Kim), jhan@krict.re.kr (J.H. Han).

http://dx.doi.org/10.1016/j.apsusc.2017.05.066
0169-4332/

growth [8] and very few occasions of proper ALD growth [14]. On the other hand, In_2O_3 ALD processes using tris-(N,N′-diisopropyl-2-dimethylamido-guanidinato)indium/H_2O and diethyl[bis(trimethylsilyl)amido]indium/H_2O resulted in growth rates of 0.04 and 0.07 nm/cycle at deposition temperatures of 240 and 200 °C, respectively [6,16]. This leads to the fact that the development of highly reactive In-precursors with sufficient volatility is essential to achieve reasonable growth rates.

Again, in attempts to increase the growth rate of In_2O_3 by ALD, stronger oxidising reactants such as O_3 and O_2 plasma can be used, but this does not always assure higher growth rates. Cyclopentadienyl-based In-precursor with O_3 yielded a high growth rate of 0.13–0.2 nm/cycle and good film conformality over a nanoporous anodic aluminum oxide membrane, while it resulted in almost no film growth when reacted with H_2O [8]. In contrast, Ramachandran et al. reported the successful growth of In_2O_3 films with excellent properties using $In(tmhd)_3$, but a low growth rate of 0.014 nm/cycle was achieved over a wide deposition temperatures of 100–400 °C even with the use of O_2 plasma as reactant [9]. Moreover, the use of such strong oxidizing reactants could result in the reduction of intrinsic electron donors such as oxygen vacancies, consequently producing rather resistive In_2O_3 films as observed by some groups [4,8]. Another important requirement in developing In-precursor is a low melting temperature to achieve liquid precursors at room temperature. Generally, for industrial applications, liquid precursors are preferred because solid compounds can cause numerous problems including powder contamination in the ALD chamber and difficulty in a reproducible supply of the precursor vapor. To this end, reports have been made on the synthesis of liquid In-precursor and their application in In_2O_3 ALD processes [15]. Maeng et al. demonstrated In_2O_3 ALD processes using liquid In-precursors [3-(dimethylamino)propyl]dimethylindium (DADI) and diethyl[bis(trimethylsilyl)amido]indium. These processes led to high growth rates of 0.06–0.07 nm/cycle, high carrier concentration of $\sim 10^{20}$–10^{21} cm^{-3}, and low resistivity of $2 \times 10^{-4} - 5 \times 10^{-5}$ Ω cm [4,16].

In this paper, we demonstrate In_2O_3 ALD process using liquid In-precursor, dimethyl(*N*-ethoxy-2,2-dimethylcarboxylicpropanamide)indium ($Me_2In(EDPA)$), in combination with H_2O as reactant. Recently authors reported the synthesis of novel $Me_2In(EDPA)$, and demonstrated the In_2O_3 PEALD process using $Me_2In(EDPA)$ with O_2 plasma as oxidant [17]. However, the application of the deposited In_2O_3 film was limited to semiconducting channel layer for thin film transistor as it showed moderate electron concentration levels of 10^{17}–10^{18} cm^{-3}, which is considerably lower than those from other In_2O_3 ALD films [4,14,16]. Here we successfully achieved In_2O_3 ALD growth using $Me_2In(EDPA)/H_2O$ chemistry, and investigated the growth behavior at stage temperatures of 150–300 °C. In addition, the chemical, physical, optical, and electrical properties of the deposited In_2O_3 films were evaluated.

2. Experimental

The In_2O_3 films were grown by ALD in a traveling wave type 4-inch chamber (Atomic-Class, CN-1) using liquid $Me_2In(EDPA)$ and deionized H_2O. Various substrates including *p*-type bare silicon and quartz substrates were used to evaluate the growth behavior and film characteristics. The base and process pressures were 3×10^{-3} and 3×10^{-1} torr, respectively. The deposition temperature of In_2O_3 film was varied from 150 to 300 °C. The In-precursor was kept in a stainless steel bubbler type canister at a temperature of 70 °C and the gas delivery line was heated to 80 °C to prevent condensation of the source material. Introduction of the In-precursor into the chamber was aided by Ar carrier gas at a flow rate of 100 sccm. The deionized H_2O was kept at ~10 °C and delivered by its own vapor pressure without carrier gas. The ALD of In_2O_3 was conducted by repeating alternative pulse of $Me_2In(EDPA)$ and H_2O gases onto the substrate. In one complete ALD cycle, the In-precursor and H_2O vapor were pulsed for 10 and 5 s, respectively, separated by 15-s Ar purge; thus 10 s–15 s–5 s–15 s. The thickness and refractive index of In_2O_3 films were estimated by spectroscopic ellipsometry (SE, Horiba Jobin Yvon UVISEL) at an angle of 70° using new amorphous model which is derived from the Forouhi-Bloomer dispersion formula. X-ray fluorescence measurement (XRF, ARLQUANT'X, Thermo Fisher Scientific) was conducted to determine the In areal density and verify surface saturated growth conditions. Electrical properties of the In_2O_3 films were investigated with a Hall effect measurement instrument (HMS-5000, Ecopia). Crystallinity of the deposited In_2O_3 films and their preferred orientation were determined by high resolution X-ray diffraction analysis (DMax–2200 V, Rigaku) using the glancing angle X-ray diffraction (GAXRD) mode. X-ray photoelectron spectrometer (XPS, K-Alpha, Thermo Scientific) equipped with a monochromatic Al Kα X-ray source was used to examine the chemical composition, atomic distribution, and possible impurities of the films. As the transparency of the In_2O_3 film is vital to its practical application, the optical properties including transmittance, absorbance and bandgap were also ascertained using a UV–vis spectrometer (UV-2550, Shimadzu). Finally, morphology of the deposited films was investigated using a field emission scanning electron microscope (FESEM, Sigma HD, Carl Zeiss).

3. Results and discussion

Prior to the complete ALD cycles, half cycle experiments consisted of In-precursor pulse followed by Ar purge were carried out to confirm no thermal decomposition of the precursor at the stage temperatures of 150–300 °C. No films were deposited at all temperatures according to ellipsometry and XRF measurements, indicating that the In-precursor remained stable up to high temperatures of 300 °C. Full ALD cycles were then conducted by varying the $Me_2In(EDPA)$ pulse time from 1 to 15 s at a fixed H_2O pulse time of 5 s at 300 °C. Each In-precursor and H_2O pulse step was separated by 15-s Ar purge to prevent gas mixture or CVD-like growth. Fig. 1(a) depicts the changes in the film thickness and In areal density for 100 ALD cycles with increasing $Me_2In(EDPA)$ pulse time. A self-limiting growth was observed after 10-s $Me_2In(EDPA)$ pulse with a thickness of ~8 nm and an In areal density of 3.3 μg/cm^2. After obtaining saturated growth condition for the In-precursor pulse, the H_2O pulse time was varied while keeping the In-precursor pulse time at 10 s. The variations of In areal density in Fig. 1(b) clearly shows that saturated growth is obtained at H_2O pulse length of 4 s, and no further increase in film thickness was observed above 4 s. The In-precursor and H_2O were pulsed for 10 s and 5 s, respectively, in a complete ALD cycle, thus ALD pulse condition of 10 s–15 s–5 s–15 s was determined. Using this optimized pulse condition, In_2O_3 thin films were grown with different cycle numbers from 100 to 400 cycles as depicted in Fig. 1(c), and a very linear growth was observed, indicating layer-by-layer growth behavior with a growth rate of 0.083 nm/cycle. To determine the effect of deposition temperature on the film growth, In_2O_3 films were deposited at various temperatures from 150 to 300 °C. Notably from Fig. 1(d), the growth rate was very dependent on the deposition temperature, increasing with temperature with no obvious temperature window within which a constant growth rate is observed. The growth rate of In_2O_3 increased slowly up to 250 °C, after which an abrupt increase in growth rate was found at 300 °C. The increase in the growth rate with temperature is mostly likely due to the increased ther-

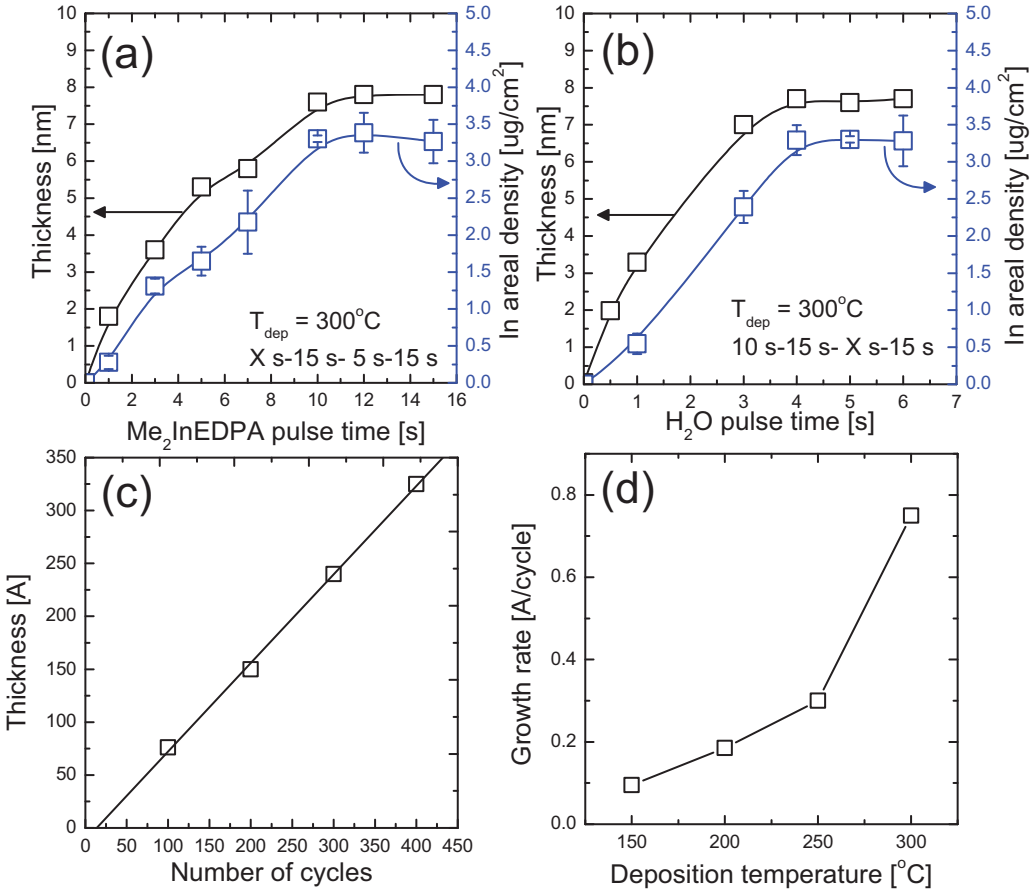

Fig. 1. The variations of the thickness and In areal density of In_2O_3 films as a function of (a) $Me_2In(EDPA)$ and (b) H_2O pulse length. (c) The variation of In_2O_3 film thickness with the number of ALD cycles. (d) The growth rates of In_2O_3 ALD at various deposition temperatures.

mal energy needed for the chemical reaction, rather than thermal decomposition of the In-precursor.

XPS was used to investigate the chemical binding state as well as the compositional distribution across the thickness of the In_2O_3 films deposited on bare silicon substrates at 150, 200, 250 and 300 °C, as shown in Fig. 2. Ar^+ ion with beam energy 2000 eV was used to sputter the samples during depth profiling and the C—C peak with binding energy of 284.5 eV detected at film surface prior to sputtering was used to calibrate all other XP spectra. Fig. 2(a)–(d) depicts the In 3d spectra of the films deposited at different temperatures. At 150 °C, the In 3d spectrum consisted of a main peak and a clear shoulder peak appearing at a lower binding energy. The spectrum was deconvoluted into two sub-peaks, In-O centered at 444.5 eV and In—In centered at 443.6 eV, which are in good agreement with reported values. [9,13,16]. The significant presence of In—In bond at 150 °C might indicate reduced surface reaction between chemisorbed precursor and H_2O reactant due to the relatively low deposition temperature. Above 150 °C, more symmetric and narrower In 3d peaks were observed at all temperatures. However, the peaks were gradually shifted towards lower binding energies from 444.1 to 443.9 eV as the deposition temperature increased from 200 to 300 °C, respectively. This shift towards lower binding energies can be attributed to the presence of oxygen vacancy [16] and is responsible for the conductivity of the films. It is worth noting that although the film deposited at 150 °C was highly oxygen deficient, it exhibited a high resistivity because of its porous and amorphous nature. The O 1 s peak was deconvoluted into three sub-peaks as presented in Fig. 2(e)–(h); thus In—O at ~530 eV, O vacancy at ~531.3 eV and O—H/C—O bonds at ~531.9 eV. At 150 °C, the shoulder peak at ~531.9 eV is suspected to be composed of O—H and/or C—O since C was detected at all etch levels, whereas above 150 °C, the shoulder peak at ~531.9 eV is expected to be mainly contributed by O—H since no C was detected in these films. The intensity of sub-peak corresponding to O—H/C—O decreased with increasing growth temperature which implies that the formation of $In(OH)_x$ in In_2O_3 was retarded at the elevated temperatures. The sub-peak intensity for O vacancy at 150 °C was slightly higher than those from 200 to 300 °C, which is consistent with observation from In 3d spectra. Depth profile plots in Fig. 2(i) and (j) confirm the oxygen deficient nature of the deposited In_2O_3 films, particularly the film deposited at 150 °C; O/In atomic ratios at 150 °C and 300 °C were 0.53 and 0.96, respectively. It also shows that the film deposited at 300 °C (as well as films deposited at 200 °C and 250 °C) had no C or N impurities while some C impurity was detected in the film deposited 150 °C during etching.

The crystallinity of the films was examined with varying growth temperature from 150 to 300 °C by GAXRD. The diffraction patterns in Fig. 3 show that the In_2O_3 films deposited at 200–300 °C were polycrystalline in nature. At these temperatures, the diffraction peaks indicated the growth of polycrystalline In_2O_3 films with cubic structure thus; [(211) at 21.7°, (222) at 30.7°, (400) at 35.7°, (332) at 42.0°, (431) at 45.8°, (440) at 51.3°, and (622) at 60.7°]. The peak intensities for In_2O_3 films remained the same above 200 °C with the (222) plane being the preferred growth orientation, which has also been identified by other reports [9,15,17]. In contrast, the film deposited at 150 °C was amorphous showing no characteristic In_2O_3 peaks.

The band gap of 15-nm thick films grown at the various temperatures was estimated by SE using Tauc plots thus; $(\alpha h\upsilon)^2$ vs $(h\upsilon)$, where α is the absorption coefficient and $h\upsilon$ is the energy

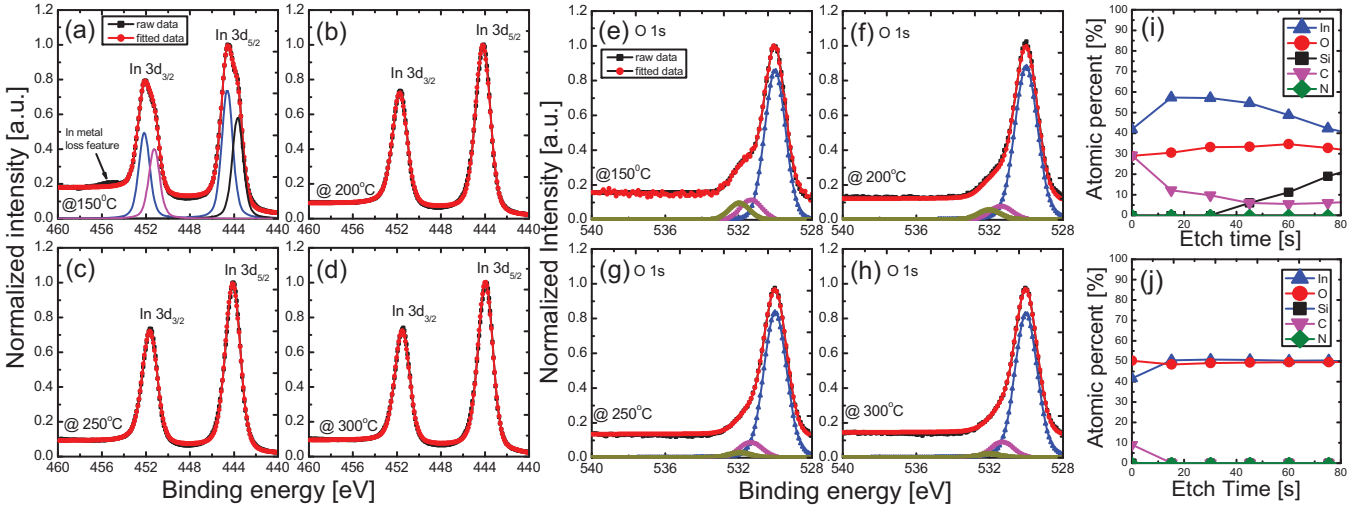

Fig. 2. (a)–(d) In 3d and (e)–(h) O 1 s XP spectra of In_2O_3 films grown at the different temperatures of 150, 200, 250, and 300 °C. XPS depth profiles of In_2O_3 films deposited at (i) 150 and (j) 300 °C.

Table 1
Carrier concentration, Hall mobility, and resistivity of In_2O_3 films deposited at various temperatures of 150, 200, 250, and 300 °C.

Deposition temperature (°C)	Film thickness (nm)	Carrier conc. (/cm^3)	Hall mobility (cm^2/V s)	Resistivity (mΩ cm)
150	15 ± 0.1	N.A.	N.A.	N.A.
	~120	2.9×10^{18}	1.1	2060
200	15 ± 0.4	1.2×10^{19}	28	7.0
250	16 ± 0.1	3.6×10^{19}	41	4.3
300	16 ± 0.2	4.8×10^{19}	32	4.1
	30 ± 0.8	7.8×10^{19}	66	1.2

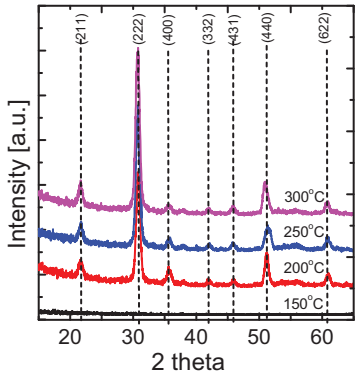

Fig. 3. GAXRD patterns of ALD In_2O_3 films deposited at 150–300 °C.

of the incident light as shown in Fig. 4(a). An extrapolation of Tauc plots revealed that films grown at 200–300 °C showed similar band gap of 3.7 eV independent of the deposition temperature, which is comparable with reported band gap of In_2O_3 films by other deposition techniques such as sputtering [18] and sol-gel method [19]. The band gap of the film deposited at 150 °C could not be estimated as the Tauc values from SE was not reliable due to the rough morphology. Fig. 4(b) shows the transmittance and absorbance spectra of the In_2O_3 films deposited on quartz substrates at 150–300 °C by UV–vis spectrometer. From the absorption edges, the estimated band gap was around 3.5–3.6 eV with the exception of the film deposited at 150 °C which exhibited the widest band gap of 3.9 eV. The porous and less dense nature of the film could have contributed to its seemingly wider band gap. The band gap values obtained from UV–vis measurements were very comparable to those estimated from SE measurements. Additionally, all films are highly transparent in the visible wavelength range with transmittance over 94%. Interestingly, the film deposited at 150 °C with the widest band gap showed a lower transmittance similar to the 200 °C sample. We suspect that the rough morphology of the films deposited at 150 °C increased the diffused reflectance at the film surface and lowered the total transmittance of the film. In the inset of Fig. 4(b), the refractive index of the films measured at λ = 550 nm increased with deposition temperature from 1.7 at 150 °C to a relatively constant value of 1.9 above 200 °C, which is slightly lower than that of bulk In_2O_3 about 2.1 [20]. As the refractive index gives a crude insight into the density of films, the low refractive index of films deposited at 150 °C suggests the films are less dense which is obvious considering the porous morphology of the films as discussed in the next paragraph. At higher temperatures over 200 °C, the densification of films resulted in an increase in the refractive index.

The SEM images in Fig. 5 depict the morphology of the films deposited at various temperatures. Here, 15 nm-thick films were examined by SEM at a high magnification (x100,000) except for 150 °C-grown sample of which thickness is about 120 nm. Films deposited at 150 °C showed a peculiar morphology different from the morphology observed at higher temperatures. Its flake-like grains were randomly arranged with some voids as shown in Fig. 5(a). As the deposition temperature increased, the grains became flattened and densely arranged with no visible pinholes, giving smooth films as displayed in Fig. 5(b)–(d). However, the film deposited at 300 °C showed rather roughened surface morphology with triangular shape grains compared to those at 200 and 250 °C.

Electrical properties of In_2O_3 films deposited at different temperatures were ascertained from Hall measurements as shown in Table 1. At 150 °C, it was impossible to obtain any reliable Hall measurement result due to the severe voids in the 15-nm thick film. However, with a thicker film, reliable electrical property data were obtained even though the resistivity was three orders of magnitude higher than the films deposited at higher temperatures

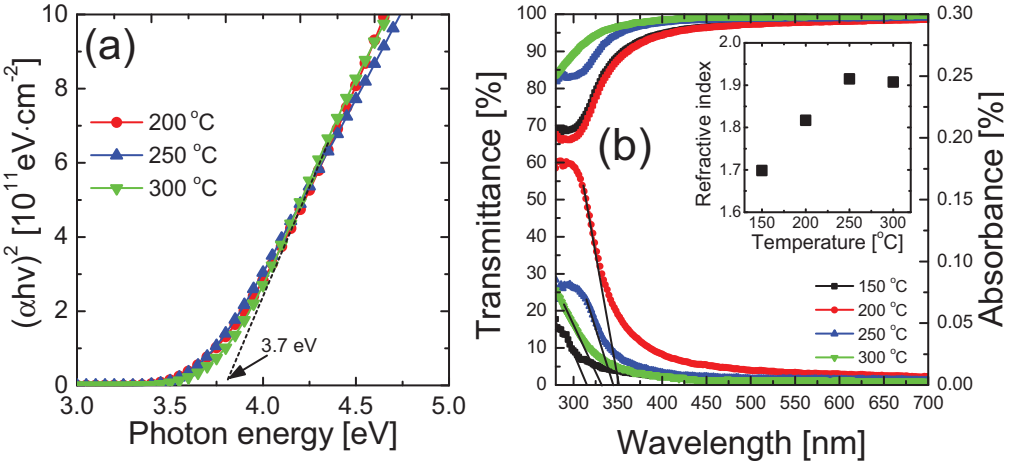

Fig. 4. (a) Tauc plot, $(\alpha h\upsilon)^2$ vs $h\upsilon$, for In_2O_3 films deposited at 200–300 °C (b) The transmittance and absorbance spectra of the films grown at 150–300 °C showing the absorption edge of each film. The inset shows the variation of refractive index for the films deposited at 150–300 °C.

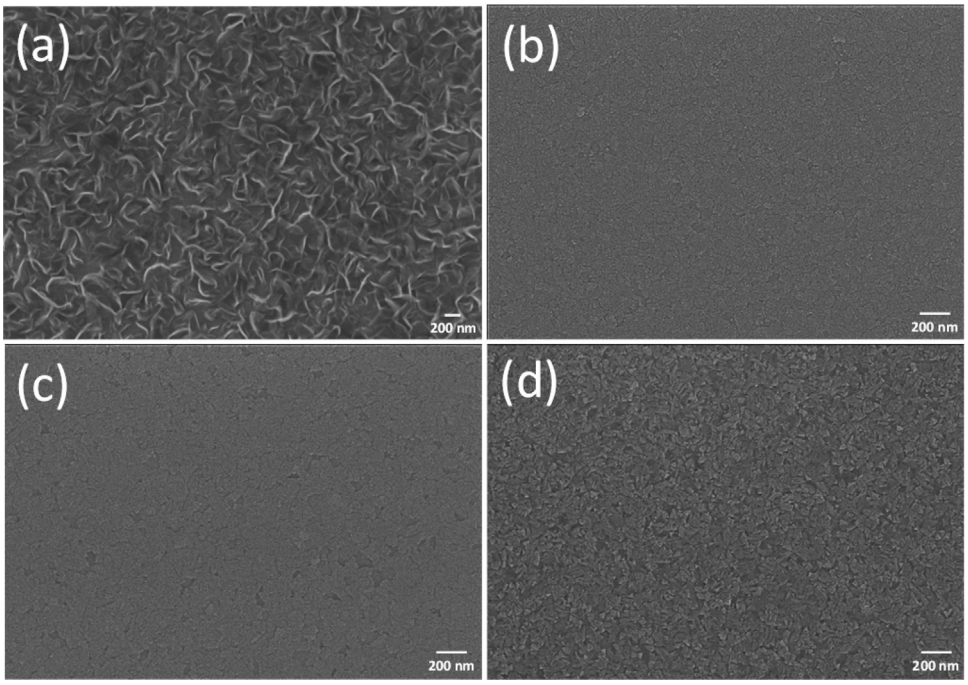

Fig. 5. The SEM plan-view images for the films deposited at (a) 150, (b) 200, (c) 250, and (d) 300 °C.

suggesting that the film was still not completely continuous. Films deposited above 150 °C showed *n*-type conductivity with carrier concentrations in the order of 10^{19}, which is comparable to values for ALD In_2O_3 films deposited with TMI/H_2O and $InCl_3$/H_2O [14,21]. The carrier concentration of In_2O_3 films increased from 1.2×10^{19} to 4.8×10^{19} cm^{-3} as the deposition temperature increased from 200 to 300 °C. This might be as a result of the creation of more oxygen vacancies and/or indium interstitials at higher temperatures, accompanied with decreased resistivity with temperature [16,22,23]. The Hall mobility of In_2O_3 films increased from 28 to 41 $cm^2/V\,s$ as the deposition temperature increased to 250 °C and then declined to 32 $cm^2/V\,s$ at 300 °C. This might be attributed to more rough surface morphology of 300 °C-grown In_2O_3 film compared to that of 250 °C-grown In_2O_3 film, which can deteriorate the electron transport property by surface scattering. The electrical parameters were much dependent on film thickness. The Hall mobility and resistivity were improved over two folds when the thickness of films deposited at 300 °C was doubled as presented in Table 1.

4. Conclusions

In conclusion, In_2O_3 thin films were grown using a liquid indium precursor; dimethyl(*N*-ethoxy-2,2-dimethylcarboxylicpropanamide)indium ($Me_2In(EDPA)$) and H_2O as reactant in an ALD process. Growth was demonstrated over a wide temperature of 150–300 °C and the growth rate increased with the deposition temperature. A high saturated growth rate of 0.083 nm/cycle was attained at 300 °C. XPS analysis revealed that films deposited at 150 °C contained significant amount of In-In bond, while films deposited at 200–300 °C were more oxygen rich and contained negligible levels of impurities. All films were crystalline in nature except for films deposited at 150 °C which were amorphous. The chemical composition, crystallinity and

morphology of the films reflected in their electrical and optical properties. Films deposited at 150 °C were very resistive whereas above 150 °C the films exhibited low resistivity of 1.2–7 mΩ cm and electron mobility of 28–66 $cm^2/V s$. The high transmittance and good electrical properties of the films deposited at high temperatures make them viable candidates for photovoltaic TCOs and for other optoelectronic applications.

Conflict of interest

The authors declare no competing financial interests.

Author contributions

The manuscript was written through contributions of all authors. All authors have given approval to the final version of the manuscript.

Acknowledgments

This work was supported by Korea Research Institute of Chemical Technology (SI1703-02, Organometallics and Device Fabrication for IT-ET Convergence Project) and the National Research Council of Science & Technology (NST) grant by the Korea government (MSIP) (No. PCS-17-02-KIST).

References

[1] P. Raghunath, M.C. Lin, Computational study on the mechanisms and energetics of trimethylindium reactions with H_2O and H_2S, J. Phys. Chem. A 111 (2007) 6481–6488.
[2] G. Shen, B. Liang, X. Wang, H. Huang, D. Chen, Z.L. Wang, Ultrathin In_2O_3 nanowires with diameters below 4 nm: synthesis, reversible wettability switching behavior, and transparent thin-film transistor applications, ACS Nano 5 (2011) 6148–6155.
[3] Q.S. Liu, W.G. Lu, A. Ma, J. Tang, J. Lin, J. Fang, Study of quasi-monodisperse In_2O_3 nanocrystals: synthesis and optical determination, J. AM. Chem. Soc. 127 (2005) 5276–5277.
[4] W.J. Maeng, D.-W. Choi, Jozeph Park, J.-S. Park, Atomic layer deposition of highly conductive indium oxide using a liquid precursor and water oxidant, Ceram. Int. 41 (2015) 10782–10787.
[5] S. Park, S. Kim, G.-J. Sun, C. Lee, Synthesis structure, and ethanol gas sensing properties of In_2O_3 nanorods decorated with Bi_2O_3 nanoparticles, ACS Appl. Mater. Interfaces 7 (2015) 8138–8146.
[6] M. Gebhard, M. Hellwig, H. Parala, K. Xu, M. Winter, A. Devi, Indium-tris-guanidinates: a promising class of precursors for water assisted atomic layer deposition of In_2O_3 thin films, Dalton Trans. 43 (2014) 937–940.
[7] G. Wang, J. Park, D. Wexler, M.S. Park, J.-H. Ahn, Synthesis characterization, and optical properties of In_2O_3 semiconductor nanowires synthesized by the chemical vapor deposition, Inorg. Chem. 46 (2007) 4778–4780.
[8] J.W. Elam, A.B.F. Martinson, M.J. Pellin, J.T. Hupp, Atomic layer deposition of In_2O_3 using cyclopentadienyl indium: a new synthetic route to transparent conducting oxide films, Chem. Mater. 18 (2006) 3571–3578.
[9] R.K. Ramachandran, J. Dendooven, H. Poelman, C. Detavernier, Low temperature atomic layer deposition of crystalline In_2O_3 films, J. Phys. Chem. C 119 (2015) 11786–11791.
[10] H.Z. Zhang, H.T. Cao, A.H. Chen, L.Y. Liang, Z.M. Liu, Q. Wan, Enhancement of electrical performance in In_2O_3 thin-film transistors by improving the densification and surface morphology of channel layers, Solid-State Electron. 54 (2010) 479–483.
[11] E.J. Tarsa, J.H. English, J.S. Speck, Pulsed laser deposition of oriented In_2O_3 on (001) InAs, MgO, and yttria-stabilized zirconia, Appl. Phys. Lett. 62 (1993) 2332.
[12] M. Ritala, T. Asikainen, M. Leskelä, J. Skarp, ALE growth of transparent conductors, J. Mater. Res. Soc. Symp. Proc. 426 (1996) 513.
[13] A.U. Mane, A.J. Allen, R.K. Kanjolia, J.W. Elam, Indium oxide thin films by atomic layer deposition using trimethylindium and ozone, J. Phys. Chem. C 120 (2016) 9874–9883.
[14] D.-J. Lee, J.-Y. Kwon, J.I. Lee, K.-B. Kim, Self-limiting film growth of transparent conducting In_2O_3 by atomic layer deposition using trimethylindium and water vapor, J. Phys. Chem. C 115 (2011) 15384–15389.
[15] J.H. Han, E.A. Jung, H.Y. Kim, D.H. Kim, B.K. Park, J.S. Park, S.U. Son, T.M. Chung, Atomic layer deposition of indium oxide thin film from a liquid indium complex containing 1-dimethylamino-2-methyl-2-propoxy ligands, Appl. Surf. Sci. 383 (2016) 1–8.
[16] W.J. Maeng, D.W. Choi, K.B. Chung, W.Y. Koh, G.Y. Kim, S.Y. Choi, J.S. Park, Highly conducting, transparent, and flexible indium oxide thin film prepared by atomic layer deposition using a new liquid precursor $Et_2InN(SiMe_3)_2$, ACS Appl. Mater. Interfaces 6 (20) (2014) 17481–17488.
[17] H.Y. Kim, E.A. Jung, G. Mun, R.E. Agbenyeke, J.S. Park, S.U. Son, D.J. Jeon, S.H.K. Park, T.M. Chung, J.H. Han, Low-temperature growth of indium oxide thin film by plasma enhanced atomic layer deposition using liquid dimethyl(N-ethoxy-2,2-dimethylpropanamido)indium for high-mobility thin film transistor application, ACS Appl. Mater. Interfaces 8 (40) (2016) 26924–26931.
[18] S. Cho, Effects of rapid thermal annealing on the properties of In_2O_3 thin films grown on glass substrate by rf reactive magnetron sputtering, Microelectron. Eng. 89 (2012) 84–88.
[19] L.N. Lau, N.B. Ibrahim, H. Baqiah, Influence of precursor concentration on the structural, optical and electrical properties of indium oxide thin film prepared by a sol-gel method, Appl. Surf. Sci. 345 (2015) 355–359.
[20] O. Medenbach, T. Siritanon, M.A. Subramanian, R.D. Shannon, R.X. Fischer, G.R. Rossman, Refractive index and optical dispersion of In_2O_3, $InBO_3$ and gahnite, Mater. Res. Bull.48 (6) 48 (2013) 2240–2243.
[21] T. Asikainen, M. Ritala, M. Leskela, Growth of In_2O_3 thin films by atomic layer epitaxy, J. Electrochem. Soc. 141 (1994) 3210–3213.
[22] H.-I. Yeom, J.B. Ko, G. Mun, S.-H. Ko Park, High mobility polycrystalline indium oxide thin-film transistors by means of plasma-enhanced atomic layer deposition, J. Mater. Chem. C 4 (2016) 6873–6888.
[23] J.C.C. Fan, J.B. Goodenough, X-ray photoemission spectroscopy studies of Sn-doped indium-oxide films, J. Appl. Phys. 48 (1977) 3524.